Chromogranin A regulates gut permeability *via* the antagonistic actions of its proteolytic peptides

Elke M. Muntjewerff[1], Kechun Tang[2], Lisanne Lutter[3,4], Gustaf Christoffersson[5,6], Mara J.T. Nicolasen[1], Hong Gao[9], Gajanan. D. Katkar[7], Soumita Das[8], Martin ter Beest[1], Wei Ying[9], Pradipta Ghosh[7,9], Sahar El Aidy[10], Bas Oldenburg[4], Geert van den Bogaart[1,10*], Sushil K. Mahata[2,9*]

[1]Department of Tumor Immunology, Radboud Institute for Molecular Life Sciences, Radboud University Medical Center, Nijmegen, the Netherlands; [2]VA San Diego Healthcare System, 3350 La Jolla Village Drive, San Diego, CA, USA; [3]Center for Translational Immunology, Utrecht University Medical Center, Utrecht, the Netherlands; [4]Department of Gastroenterology and Hepatology, Utrecht University Medical Center, Utrecht, the Netherlands; [5]Science for Life Laboratory and [6]Department of Medical Cell biology, Uppsala University, Uppsala, Sweden; [7]Departments of Cellular and Molecular Medicine, [8]Pathology, [9]Medicine, University of California San Diego, La Jolla, CA, USA; [10]Department of Molecular Immunology and Microbiology, Groningen Biomolecular Sciences and Biotechnology Institute, University of Groningen, Groningen, the Netherlands.

Author names in bold designate shared co-first authorship

Conflict of interest: The authors declare no conflict of interest.

Author contributions: E.M.M., S.K.M. and G.v.d.B designed the study. E.M.M, K.T., L.L., G.C., M.t.B., S.E.A., W.Y. and S.K.M. designed and performed the experiments. M.J.T.N., B.W., P.G., H.G., S.D., G.D.K. and L.L., contributed to the experiments. L.L. and B.O. provided donor material. E.M.M., L.L., P.G., S.K.M. and G.v.d.B wrote the manuscript and all authors participated in discussing and editing of the manuscript.

Short Title: Catestatin tightens the gut barrier

Key Words: Enteroendocrine cells, gut barrier, epithelial tight junctions, chromogranin A, catestatin

***Correspondence should be addressed to**: Sushil K. Mahata, Metabolic Physiology & Ultrastructural Biology Laboratory, Department of Medicine, University of California San Diego, 9500 Gilman Drive, La Jolla, CA 92093-0732, smahata@health.ucsd.edu or Geert van den Bogaart, [6]Department of Molecular Immunology and Microbiology, Groningen Biomolecular Sciences and Biotechnology Institute, University of Groningen, Groningen, the Netherlands, g.van.den.bogaart@rug.nl.

Grant support:

This work was supported by grants from the Veterans Affairs (I01 BX003934 to SKM), the Human Frontier Science Program (HFSP; RGY0080/2018 to G.v.d.B), the Netherlands Organization for Scientific Research (NWO-ALW VIDI 864.14.001 to G.v.d.B), and European Research Council (grant agreement No. 862137 to G.v.d.B). G.C. is supported by grants from the Swedish Research Council and the Swedish Society for Medical Research. S.E.A. is funded by is supported by a Rosalind Franklin Fellowship, co-funded by the European Union and University of Groningen, The Netherlands. E.M.M is supported by a short-term EMBO fellowship (EMBO7887).

Abstract

Background and Aims. A 'leaky' gut barrier has been implicated in the initiation and progression of a multitude of diseases, e.g., inflammatory bowel disease, irritable bowel syndrome, celiac disease, and colorectal cancers. Here we asked how Chromogranin A (CgA), a major hormone produced by the enteroendocrine cells, and Catestatin (CST), the most abundant CgA-derived proteolytic peptide, affect the gut barrier.

Methods and Results. Ultrastructural studies on the colons from Catestatin (CST: $hCgA_{352-372}$) knockout (CST-KO) mice revealed (i) altered morphology of tight (TJ) and adherens (AJ) junctions and desmosomes, indicative of junctional stress and (ii) an increased infiltration of immune cells compared to controls. Flow cytometry studies confirmed these cells to be macrophages and $CD4^+$ T cells. Gene expression studies confirmed that multiple TJ-markers were reduced, with concomitant compensatory elevation of AJ and desmosome markers. Consistently, the levels of plasma FITC-dextran were elevated in the CST-KO mice, confirming leakiness' of the gut. Leaky gut in CST-KO mice correlated with inflammation and a higher ratio of Firmicutes to Bacteroidetes, a dysbiotic pattern commonly encountered in a multitude of diseases. Supplementation of CST-KO mice with recombinant CST reversed this leakiness and key phenotypes. Supplementation of CgA-KO mice with either CST alone, or with the pro-inflammatory proteolytic CgA fragment pancreastatin (PST: $CgA_{250-301}$) showed that gut permeability is regulated by the antagonistic roles of these two peptide hormones: CST reduces and PST increases leakiness.

Conclusion. We conclude that the enteroendocrine cell-derived hormone, CgA regulates gut permeability. CST is both necessary and sufficient to reduce the leakiness. CST acts primarily *via* antagonizing the effects of PST.

82 **What you need to know**

83 **Background and Context.** The intestinal barrier is disrupted in many intestinal diseases
84 such as Crohn's disease. Chromogranin A (CgA) is produced by enteroendocrine cells in
85 the gut. CgA is proteolytically cleaved into bioactive peptides including catestatin (CST)
86 and pancreastatin (PST). The role of CgA in the gut is unknown.

87 **New findings.** CgA is efficiently processed to CST in the gut and this processing might
88 be decreased during active Crohn's disease. CST promotes epithelial barrier function and
89 reduces inflammation by counteracting PST.

90 **Limitations.** The complete mechanism of intestinal barrier regulation by CST likely
91 involves a complex interplay between the enteroendocrine system, metabolism, the
92 epithelium, the immune system and the gut microbiota.

93 **Impact.** Our findings indicate that CST is a key modulator of the intestinal barrier and
94 immune functions that correlates with disease severity of Crohn's disease. CST could be
95 a target for therapeutic interventions in Crohn's disease.

96 **Introduction**

97

98 The intestinal tract harbors 10^3-10^{11} bacteria/ml[1], that in aggregate, can constitute >1 g
99 of endotoxin[2]. Endotoxins stimulate immune cells in the lamina propria, which can trigger
100 mucosal inflammation[3]. Two factors can increase such inflammation: (i) luminal
101 dysbiosis[4] and (ii) gut barrier defects. The gut barrier is comprised of a surface mucus
102 layer which separates intact bacteria and large particulates from the mucosa[5] and the
103 colonic epithelium which provides a physical and immunological barrier separating the
104 body from the luminal contents (e.g., dietary antigens, a diverse intestinal microbiome,
105 and pathogens)[6-8]. Mucosal homeostasis is maintained by the delicate and complex
106 interactions between epithelial cells, immune cells, and luminal microbiota[6].

107 The gastrointestinal epithelium not only forms the body's largest interface with the
108 external environment but also establishes a selectively permeable epithelial barrier; it
109 allows nutrient absorption and waste secretion while preventing the entry of luminal
110 contents. The epithelial barrier is regulated by a series of intercellular junctions between
111 polarized cells: an apical tight junction (TJ), which guards paracellular permeability, the
112 subjacent adherens junction (AJ) and the desmosomes; the AJs and desmosomes do not
113 seal the paracellular space but provide essential adhesive and mechanical properties that
114 contribute to barrier functions[7].

115 The permeability of the barrier is regulated by numerous factors. For example,
116 TNF-α increases flux of larger molecules, such as proteins and other macromolecules,
117 through the leak pathway, and IL-13 selectively enhances the flux of small molecules and
118 ions via the pore pathway[9]. TNF-α plays crucial roles in the caveolin-1-mediated
119 internalization of occludin (OCLN), which elevates gut permeability. Conversely,
120 overexpression of OCLN alleviates the cytokine-induced increase in gut permeability[10].
121 IFN-γ increases gut permeability by reducing the expression of tight junction protein 1
122 (TJP1) and OCLN as well as by modulating acto-myosin cytoskeleton interactions with
123 TJ proteins[11]. The simultaneous presence of TNF-α and IFN-γ deteriorates intestinal
124 integrity by dissociating TJ proteins[12].

125 Here we show that the permeability of the gut barrier is finetuned by a major gut
126 hormone, Chromogranin A (CgA). CgA is an acidic secretory proprotein[13-15] that is

127 abundantly expressed in enteroendocrine cells (EEC) of the gut and serves as a common
128 marker for the EEC of the gut[16,17]. As a proprotein, CgA gives rise to several peptides of
129 biological importance: catestatin (CST: $hCgA_{352-372}$)[18], pancreastatin (PST: $hCgA_{250-301}$)[19],
130 WE14[20], vasostatin[21], and serpinin[22]; we show that CST is abundantly processed in the
131 gut. Unexpectedly, we found, that CgA regulates the gut permeability via the antagonistic
132 actions of its two peptides, PST and CST; while PST is a pro-inflammatory, pro-
133 obesigenic and anti-insulin peptide[23] which loosens the barrier, CST acts as anti-
134 inflammatory, antiobesigenic, anti-microbial, and proinsulin peptide[15,24-27] that appears to
135 be necessary and sufficient to neutralize the actions of PST and tighten the barrier. Using
136 knockout (KO) mice in conjunction with recombinant proteins, we show that CST exerts
137 its actions *via* counteracting PST.
138

Material and Methods

Mice. Male WT, CST-KO and CgA-KO mice (3 weeks old) on C57BL/6 background were kept in a 12 hr dark/light cycle on normal chow diet (NCD: 13.5% calorie from fat; LabDiet 5001, Lab Supply, Fort Worth, TX). All mouse studies were approved by the UCSD and Veteran Affairs San Diego Institutional Animal Care and Use Committees and conform to relevant National Institutes of Health guidelines. Experiments were conducted in a blinded fashion whenever possible. For terminal procedure, mice were deeply anesthetized (assessed by pinching toe response) with isoflurane followed by harvesting of tissues. Euthanasia was achieved through exsanguination. For rescue experiments with exogenous CST and PST, mice were injected intraperitoneally with CST (2 μg/g body weight) and/or PST (2 μg/g body weight) at 9:00 AM for 2-4 weeks before collecting feces or harvesting tissues.

Determination of CgA, CST, and calprotectin in colon. Mouse EIA kits from CUSABIO (CUSABIO Technology LLC, Houston, TX) were used to determine CgA (CSB-EL005344MO), CST (CSB-E17357m), and calprotectin (CSB-EQ013485MO).

Gut permeability assay. Fluorescein isothiocyanate conjugated dextran (FITC-dextran-FD4) (MilliporeSigma, St. Louis, MO) was administered (44 mg/100 g body weight) to 8 hr fasting mice by oral gavage followed by collection of blood after 4 hr of administration from the heart under deep isloflurane anesthesia[28]. Plasma concentration of FITC was determined by comparison of fluorescence signals with a FITC-dextran standard curve.

Measurement of tissue and plasma cytokines. Tissue and plasma cytokines were measured using U-PLEX mouse cytokine assay kit (Meso Scale Diagnostics, Rockville, MD) via the manufacturer's protocol.

Determination of CgA and CST levels in human plasma. EDTA-plasma was collected from patients with Crohn's disease (N=89) and ulcerative colitis (N=101) (Supplementary table 1) and healthy controls (N=50). Intestinal inflammation was assessed by

170 colonoscopy. A flare-up was defined as histological and endoscopic disease activity,
171 whereas remission entailed absence of endoscopic inflammation and histological disease
172 activity. Informed consent was obtained and the study was conducted in accordance with
173 the Institutional Board Review of the University Medical Center Utrecht (approval number
174 NL35053.041.11 & 11-050). EDTA-plasma from healthy controls (Supplementary table 2)
175 was obtained from the Mini Donor Service at the University Medical Center Utrecht.
176 Samples were thawed and diluted 50-times with extraction buffer (PBS with 0.5% Tween
177 and 0.05% sodium azide), thoroughly vortexed followed by incubation at 4°C for 20 min
178 on a rolling device. Afterwards samples were centrifuged at 760 ×g for 20 min at 4°C and
179 the supernatant was collected for analysis. Samples were collected in compliance with
180 the Declaration of Helsinki. EDTA plasma was used to quantify CgA and CST using ELISA
181 (CUSABIO CSB-E17355h, CSB-E09153h).
182
183 **Transmission Electron Microscopy (TEM) and morphometric analysis.** To displace
184 blood and wash tissues before fixation, mice were cannulated through the apex of the
185 heart and perfused with a Ca^{2+} and Mg^{2+} free buffer composed of DPBS and 9.46 mM
186 KCl as described[29]. Fixation, embedding, sectioning and staining were done as
187 described[29]. Grids were viewed using a JEOL JEM1400-plus TEM (JEOL, Peabody, MA)
188 and photographed using a Gatan OneView digital camera with 4×4k resolution (Gatan,
189 Pleasanton, CA). Morphometric analyses of the dense core vesicles were determined as
190 described[30].
191
192 **Flow cytometry analysis.** Isolated colon cells from digested mouse colon were stained
193 with fluorescence-tagged antibodies to detect macrophages ($CD45^+CD11b^+Emr1^+$) and
194 helper T cells ($CD45^+CD4^+$). Data were analyzed using FlowJo.
195
196 **Microbiome analysis.** DNA was extracted from cecum using the Zymobiomics miniprep
197 kit. Isolated DNA was quantified by Qubit (ThermoFisher Scientific). DNA libraries were
198 prepared using the Illumina Nextera XT library preparation kit. Library quantity and quality
199 was assessed with Qubit and Tapestation (Agilent Technologies). Libraries were
200 sequenced on Illumina HiSeq platform 2×150bp. Unassembled sequencing reads were

201 directly analyzed by CosmosID bioinformatics platform (CosmosID)[31-33] for multi-kingdom
202 microbiome analysis and profiling of antibiotic resistance and virulence genes and
203 quantification of organism's relative abundance. This system utilizes curated genome
204 databases and a high-performance data-mining algorithm that rapidly disambiguates
205 hundreds of millions of metagenomic sequence reads into the discrete microorganisms
206 engendering the particular sequences. Data mining, interpretation and comparison of
207 taxonomic information from the metagenomic datasets were performed using Calyspo
208 Bioinformatics software V.8.84.
209
210 **Real Time PCR.** Total RNA from colon tissue was isolated using RNeasy Mini Kit and
211 reverse-transcribed using qScript cDNA synthesis kit. cDNA samples were amplified
212 using PERFECTA SYBR FASTMIX L-ROX 1250 and analyzed on an Applied Biosystems
213 7500 Fast Real-Time PCR system. Primer sequences are in Supplementary table 3. All
214 PCRs were normalized to *Rplp0*, and relative expression levels were determined by the
215 $\Delta\Delta C_t$ method as described[26].
216
217 **Statistics.** Statistics were performed with PRISM 8 (version 8.4.3; San Diego, CA). Data
218 were analyzed using either unpaired two-tailed Student's *t*-test for comparison of two
219 groups or one-way or two-way analysis of variance for comparison of more than two
220 groups followed by Tukey's *post hoc* test if appropriate. All data are presented as mean
221 ± SEM and significance were assumed when $p<0.05$.
222
223
224

225 **Results**

226

227 **CgA is extensively processed to CST.** To study the role of CgA and its peptides in the
228 regulation of the gut barrier, we used systemic CgA-KO (deletion of exon 1 and ~1.5 kbp
229 proximal promoter, thereby completely inactivating the *Chga* allele)[34] and CST-KO mice
230 (the 63 bp CST domain of CgA was deleted from Exon VII of the *Chga* gene)[35]. We
231 analyzed the function and morphology of the gut barrier in CST-KO mice. We used
232 transmission electron microscopy (TEM) to resolve the ultrastructure of EECs and to
233 evaluate the subcellular compartment where hormones are stored and released, i.e.,
234 dense core vesicles (DCVs). While DCV numbers were reduced in both CgA-KO and
235 CST-KO mice, DCV areas were smaller in CgA-KO mice but larger in CST-KO mice (Fig.
236 1A-B). WT colon showed a lower concentration of CgA (average 0.019 nmol/mg protein)
237 than of CST (average 0.37 nmol/mg protein), indicating extensive processing of CgA to
238 CST (Fig. 1C). As anticipated, in CST-KO mice the levels of CgA in the colon were similar
239 to that in WT mice, but those of CST were undetectable (Fig. 1C). Consistent with
240 enhanced processing of CgA, we found increased expression of the proteolytic enzymes
241 Cathepsin L (*Ctsl*, which cleaves CST from CgA) and Plasminogen (*Plg*, the precursor of
242 plasmin, which is involved in CgA processing) in CST-KO and CgA-KO, respectively (Fig.
243 1D)[36-39].

244 Because the processing of CgA to CST is compromised in several diseases [40-44],
245 we determined plasma CgA and CST levels in patients with Crohn's disease and with
246 ulcerative colitis, both with active disease and in remission (Fig. 1E; Supplementary Fig.
247 1). In line with previous findings[45-50], we found higher CgA levels in plasma of patients
248 with active Crohn's disease but not in patients in remission. In contrast, we found higher
249 plasma CST levels in Crohn's disease regardless of disease activity, indicating that the
250 processing of CgA to CST is more efficient in disease activity.

251

252 **CST-KO mice have a 'leaky' gut.** Ultrastructural evaluation of the gut epithelium showed
253 that the TJs, AJs and desmosomes are significantly different in CST KO mice compared
254 to wild-type (WT); the TJs, AJs and desmosomes were elongated and widened (Fig. 2A-
255 B). Gene expression studies show reduced expression of multiple TJ-markers such as

256 *Ocln* (regulates the paracellular pathway), *Marveld2* (modulates macromolecular flux),
257 *F11r* (regulates gut permeability), and *Tjp1* (modulates leak pathway flux), with
258 concomitant compensatory elevated expression of AJ genes including alpha-E-Catenin
259 (*Ctnna1;* regulates gut permeability by binding to Tjp1), Cadherin-associated protein
260 (*Ctnnb1;* creates an inflammatory microenvironment), Cadherin 1 (*Cdh1,* mediates
261 homotypic intercellular adhesions) (Fig. 2C). Increased plasma FITC-dextran in the CST-
262 KO mice (Fig. 2D), confirmed leakiness of the gut. Consistent with increased leakiness,
263 we found increased expression of *Cldn2* (Fig. 2C), a specific claudin that is known to
264 increase the paracellular flux (pore pathway) of cations (e.g., Na^+) and water[51].
265
266 **The leaky gut in CST-KO mice is accompanied by mucosal inflammation and**
267 **dysbiosis.** Because increased gut permeability is often associated with mucosal
268 inflammation, we investigated the immune cell populations in the colons of CST-KO mice.
269 As expected, increased leakiness in the CST-KO colon was associated with an increased
270 abundance of immune cells (Fig. 3A). Flow cytometry confirmed increased abundance of
271 macrophages ($CD45^+11b^+Emr1^+$) and helper $CD4^+$ T cells (Fig. 3B). CST-KO mice show
272 increased expression of the following proinflammatory genes: tumor necrosis factor alpha
273 (*Tnfa*), interferon gamma (*Ifng*), chemokine CXC motif ligand 1 (*Cxcl1* aka *Kc/Gro1*),
274 chemokine CC motif ligand 2 (*Ccl2* aka *Mcp1*), egg-like module-containing mucin-like
275 hormone receptor 1 (*Emr1* aka *F4/80*), integrin alpha-M (*Itgam* aka *Cd11b*), and integrin
276 alpha-X (*Itgax* aka *Cd11c*) (Fig. 3C). Increased expression of *Tnfa, Ifng, Cxcl1*, and *Ccl2*
277 genes correlated with increased protein levels (Fig. 3D). Upregulation of proinflammatory
278 cytokines is in line with prior work demonstrating a positive correlation of IFN-γ[52] and TNF-
279 α[53] with intestinal leakiness. The decreased expression of anti-inflammatory cytokines,
280 such as interleukin 4 (*Il4*) and interleukin 10 (*Il10*), in CST-KO mice is also in congruence
281 with the reported role of anti-inflammatory cytokines in gut permeability (Fig. 3E)[54]. The
282 decreased *Il10* mRNA levels correlated with a decreased protein level of IL-10 (Fig. 3F).
283 Furthermore, the expression of *S100a9* gene and protein levels (forming Calprotectin in
284 complex with S100a8) were increased in colon of CST-KO mice (Fig. 3G); increased
285 Calprotectin, a protein secreted by activated neutrophils and macrophages, has been
286 shown to increase intestinal permeability[55-57].

287 Because a leaky gut may either cause or be the consequence of altered luminal
288 microbes[58,59], we investigated whether the microbial population in CST-KO mice was
289 altered. We found that the microbiome in CST-KO mice was indeed quite different in
290 composition than its WT littermates (Fig. 4; Supplementary Fig. 2). Most prominently,
291 CST-KO mice showed a higher ratio of Firmicutes to Bacteroidetes (Fig. 4B-D), which is
292 opposite to the decreased ratio observed in WT mice intra-rectally infused with CST[60],
293 and supports the idea that a low ratio of Firmicutes to Bacteriodetes could be beneficial
294 to dampen intestinal inflammation[60,61].
295 That the leaky gut of CST-KO mice is inflamed and harbors dysbiotic luminal
296 contents implies that CST is required for maintaining gut barrier integrity and preventing
297 dysbiosis and gut inflammation. This is important because a "leaky gut"[62], dysbiosis[63],
298 and hyperactivated immunity[64] are all well known to play a role in inflammatory bowel
299 disease (IBD). It is also consistent with others' observation that administration of
300 exogenous CST can ameliorate colitis in mice[65,66].
301
302 **CST is sufficient to tighten the leaky gut barrier in CST-KO mice and reduce**
303 **inflammation.** To test whether CST is sufficient to regulate gut permeability, we
304 supplemented CST-KO mice with recombinant CST (2 μg/g body weight once daily for
305 15-30 days, IP), which reversed gut leakiness and the associated abnormalities such as:
306 (i) reduced plasma FITC-dextran even lower than WT level (Fig. 5A), (ii) increased
307 expression of *Ocln*, *Marveld2*, *F11r*, *Tjp1, and Dsg2* (Fig. 5B&D), (iii) decreased
308 expression *of Cldn2*, *Ctnna1*, *Ctnnb1*, and *Cdh1* (Fig. 5B-C), (iv) decreased expression
309 of proinflammatory genes (*Tnfa*, *Ifng*, *Cxcl1, Ccl2, Emr1*, *Itgam*, and *Itgax)* (Fig. 5E*)*, and
310 proteins (Tnf-α, Ifn-γ, Cxcl1, Ccl2) (Fig. 5F), (v) increased expression of anti-inflammatory
311 genes (*Arg1*, *Il4*, *Tgfb1*, *Il10*, *Mrc1*, *Clec7a*, and *Clec10a*) (Fig. 5G), and protein (Il10)
312 (Fig. 5H), (vi) decreased expression of calprotectin gene (subunit *S100a9)* and protein
313 levels (Fig. 5I). These findings demonstrate that CST is not only required for the integrity
314 of the gut barrier but is also sufficient to maintain the integrity of this barrier during
315 homeostasis.
316

317 **The permeability of the gut is intact in CgA-KO mice.** Next, we carried out the gut
318 barrier studies in CgA-KO mice, which not only lack CST, but also lack all other peptides
319 derived from CgA. Ultrastructural studies showed no structural changes in TJ, AJ and
320 desmosomes in CgA-KO mice compared to WT mice (Fig. 6A). To our surprise, we found
321 that despite the absence of CST in these mice, gut permeability was not increased, as
322 assessed by FITC-dextran uptake (Fig. 6B); if anything, the barrier was even tighter than
323 WT control mice. This decreased permeability was not accompanied by changes in CgA-
324 KO mice in genes coding for components of TJ, AJ and desmosomes, except that *Ocln*
325 and *Dsg2* gene expression were decreased in CgA-KO mice compared to WT mice (Fig.
326 6C). Likewise, proinflammatory gene and protein expressions were not affected in CgA-
327 KO mice (Fig. 6D-E). However, increased expression of anti-inflammatory genes and
328 protein in CgA-KO mice was observed (Fig. 6F-G). Decreased expression of calprotectin
329 protein is also consistent with decreased gut permeability (Fig. 6H). Compared to CST-
330 KO mice, Firmicutes and Bacteroidetes bacteria populations in CgA-KO mice were more
331 comparable to WT mice (Fig. 7A; Supplementary Fig. 2). These findings suggest that CST
332 is not essential in the absence of CgA. Because a leaky and inflamed gut was seen in the
333 CST-KO mice which specifically lack the proteolytic fragment of CST, but not in CgA-KO
334 mice which lack CST and all other peptides that are generated proteolytically from CgA,
335 these findings raised the possibility that CST may be required to antagonize the actions
336 of some other peptide hormone that is also a product of CgA.
337
338 **Gut permeability is regulated by the antagonistic effects of two CgA peptides: CST**
339 **and Pancreastatin (PST).** Among the various proteolytic peptides, we hypothesized that
340 CST could be acting to balance the impact of another peptide fragment of CgA, i.e.,
341 pancreastatin (PST) (Fig. 7B). This hypothesis was guided by prior work[67] alluding to
342 PST's deleterious impact on the gut mucosa, causing macrophage infiltration and
343 inflammation. To test the nature of contribution of PST and CST on the gut barrier
344 function, we supplemented the CgA-KO mice with either CST alone (2 μg/g body weight
345 for 15 days), or PST alone (2 μg/g body weight for 15 days), or both PST and CST co-
346 administered at equimolar ratio for 15 days. CST alone did not change leakiness in CgA-
347 KO mice (Fig. 7C). By contrast, PST alone increased the leakiness in CgA-KO mice and

348 this leakiness was markedly reduced when the CgA-KO mice received both PST and CST
349 at equimolar concentration (Fig. 7C). These findings indicate that PST is sufficient to
350 increase gut permeability, and that CST is sufficient to antagonize this action. Together,
351 these data lead us to propose a working model (Fig. 7D) in which the intestinal epithelial
352 barrier is finetuned by the EECs via a major gut hormone, CgA. Our data show that CgA
353 is proteolytically processed into two peptides, CST and PST, which tighten and loosen
354 the gut barrier, respectively.
355
356
357

358 **Discussion**

359

360 The major finding in this work is the discovery of a molecular mechanism that involves a
361 major EEC-derived gut hormone that has a balanced action on the gut barrier; two
362 hormone derivatives of CgA, i.e., CST and PST, which either tighten or loosen the barrier,
363 respectively. Because CgA-KO mice had an unimpaired gut barrier, which was loosened
364 by exogenous administration of PST but not tightened by exogenous CST alone, findings
365 also indicate that the barrier-homeostatic mechanism(s) is contained within and converge
366 at a molecular level on the prohormone CgA and its processing into counteracting peptide
367 hormones. These findings are important because CST is a major peptide hormone in EEC
368 which is proteolytically produced from CgA by PC1[68], cathepsin L[39], plasmin[37] and
369 kallikrein [69]. Its abundance in the gut suggests that the permeability of the gut barrier is
370 regulated by CST.

371

372 **Antagonistic effects of PST and CST determine gut permeability.** CgA is unique in
373 having peptide domains that antagonize several functions including inflammation (CST
374 suppresses while PST promotes)[23,26], obesity (CST inhibits while PST stimulates)[23,26] and
375 sensitivity to insulin (CST increases while PST diminishes)[23,26,70,71]. Since CgA-KO mice
376 lack both CST and PST, and we observed increased permeability in CST-KO mice and
377 decreased permeability in CgA-KO mice, we reasoned that these opposing phenotypes
378 are probably caused by the lack of PST in the CgA-KO mice. Indeed, the increased
379 permeability in PST-treated CgA-KO mice and its reversal by co-treatments of PST and
380 CST lead us to conclude that CST promotes the epithelial barrier function by
381 counteracting PST.

382

383 **CST tightens the gut barrier by its anti-inflammatory effect on the macrophages.**
384 While PST exerts deleterious impact on the gut mucosa, causing macrophage infiltration
385 and inflammation[67], we found that lack of CST caused an increased expression of
386 proinflammatory genes and proteins and treatment of CST-KO mice with CST reversed
387 expression of those genes and proteins. Our findings are in congruence with the existing
388 literature which showed increased TJ permeability in presence of increased

389 proinflammatory cytokines such as TNF-α, IL-1β, and IFN-γ[52,53,72]. Of course, a reduced
390 gut barrier function will facilitate the leakage of microbial components such as
391 lipopolysaccharide (LPS) and peptidoglycan (PGN) from the lumen of the gut into the
392 tissues, where they can bind to pattern recognition receptors and activate the immune
393 system. In turn, the increased inflammation can result in further leakage of the gut. For
394 instance, myosin light chain kinase (MLCK) plays critical roles in cytokine-mediated TJ
395 regulation by disrupting the interaction between TJ proteins and the actin-myosin
396 cytoskeleton[73,74] leading to damage of the TJ scaffold, which is crucial for the
397 maintenance of barrier integrity[74]. Inflammatory cytokine-induced intestinal barrier loss is
398 also believed to be due to endocytosis of TJ proteins[10], which also requires MLCK
399 transcription and activity at the TJ. In addition to the above mechanisms, TNF-α
400 suppresses TJ barrier function by decreasing expression of TJP1 protein, increasing
401 expression of CLDN2, and activating the NF-κB pathway[75]. IL-6 also increases
402 expression of CLDN2[76]. Besides TJP1, IFN-γ also reduces expression of OCLN in an
403 AMPK-dependent pathway to increase barrier permeability[11].
404
405 **Emergence of CST as an important gastrointestinal peptide hormone.** The present
406 study unequivocally demonstrates that CST is a key regulator of gut permeability since
407 the absence of CST (CST-KO) is accompanied by dysbiosis, increased gut permeability,
408 increased infiltration of macrophages and $CD4^+$ T cells and higher local inflammatory
409 gene and protein expression with the substitution of CST-KO mice with CST reversing
410 many of the above abnormalities. Do gut hormones simulate the actions of CST? While
411 Cholecystokinin (CCK) decreases mucosal production of proinflammatory cytokines
412 induced by LPS and increases the expression of seal forming TJ proteins (OCLN, CLDN
413 and JAM-A)[77], Ghrelin ameliorates sepsis-induced gut barrier dysfunction by activation of
414 vagus nerve via central ghrelin receptors[78] as well as by decreasing production of TNF-α
415 and IL-6[79]. Glucagon-like peptide 1 (GLP-1) has also been shown to decrease
416 inflammation of enterocytes[80]. Vasoactive intestinal peptide, a neuropeptide found in
417 lymphocytes[81], mast cells[82], and enteric neurons of the gastrointestinal tract regulates
418 both epithelial homeostasis[83] and intestinal permeability[84]. The multitude of effects of CST

419 on gut physiology and their recapitulation by these well-investigated gut hormones
420 establishes CST as an important gastrointestinal peptide hormone.
421
422 **CST and CgA regulate gut barrier function.** CST-KO mice (loss of barrier integrity) are
423 insulin-resistant on normal chow diet[26] and CgA-KO mice (intact barrier integrity) are
424 supersensitive to insulin in both normal chow and on high fat diet[23,70]. Could metabolic
425 endotoxemia explain the above phenotypes? Besides gastrointestinal peptide hormones
426 and neuropeptides, TJ homeostasis is altered by proinflammatory cytokines, pathogenic
427 bacteria, and pathological conditions like insulin resistance and obesity. Firmicutes (e.g.,
428 *Lactobacillus*, *Clostridium*, and *Enterococcus*) and Bacteroidetes (e.g., *Bacteroides*)
429 constitute the major bacterial phyla in the gut[85]. Enteric pathogenic bacteria such as
430 *Escherichia coli* and *Salmonella typhimurium* alter the intestinal epithelial TJ barrier and
431 cause intestinal inflammation[86]. LPS alters expression and localization of TJ proteins such
432 as TJP1 and OCLN[87]. Since high fat diet-induced insulin-resistant mice and patients with
433 obesity or diabetes display elevated levels of Firmicutes and Proteobacteria compared to
434 the beneficial phylum Bacteroidetes[61], it is conceivable that dysbiosis (i.e., increased
435 Firmicutes and decreased Bacteroidetes) in CST-KO mice is due to their resistance to
436 insulin. This is further supported by the fact that *Akkermansia muciniphila*, which
437 regulates intestinal barrier integrity, is less abundant in diabetic individuals[88].
438 Furthermore, the daily administration of *A. muciniphila* is known to mitigate high fat-
439 induced gut barrier dysfunction [89]. Conversely, metabolic endotoxemia, resulting from the
440 loss of barrier integrity, contributes to insulin resistance and obesity[90,91]. The intact barrier
441 function in CgA-KO mice could thus be due to their heightened sensitivity to insulin.
442 Human calprotectin, a 24 kDa dimer, is formed by S100A8 and S100A9 monomers
443 and released from neutrophils and monocytes. In fact, this calprotectin complex
444 constitutes up to 60% of the soluble proteins in the cytosol of neutrophils[92] and fecal
445 calprotectin levels serve as a marker of intestinal inflammation[93,94]. Because of the
446 positive correlation between calprotectin concentration in gut lavage fluid and intestinal
447 permeability[95], calprotectin levels are also used to assess intestinal permeability.
448 Increased calprotectin levels have been reported to increase intestinal permeability [56].

449 Therefore, increased gene and protein expressions in the colon of CST-KO mice are in
450 line with the increased permeability in CST-KO mice.
451
452 **Impact of CgA and CST in inflammatory bowel diseases.** Elevated plasma CST levels
453 in patients suffering from Crohn's disease both in disease remission and flare-up as
454 compared to elevated precursor CgA in Crohn's disease flare-ups only suggests that
455 while CgA is generally upregulated in Crohn's disease, it is only efficiently processed to
456 CST during disease remission. Previous studies revealed higher plasma CgA levels
457 during flare-ups as compared to ulcerative colitis and Crohn's disease patients in
458 remission[45]. These and our findings suggest a proteolytic switch, where CgA and CST
459 are excessively produced in Crohn's disease regardless of the disease state, but CgA is
460 converted more into the anti-inflammatory CST in quiescent Crohn's disease. The gut
461 barrier dysfunction in CST-KO mice is reminiscent of active Crohn's disease, because the
462 gut permeability provided by cell-cell junctions is generally diminished in IBD patients[96].
463 Based on our findings, we hypothesize that the higher levels of CST during Crohn's
464 disease remision promote anti-inflammatory responses and aid restoration of epithelial
465 cellular junctions.
466
467
468
469

Data and materials availability: All data is available in the main text or the supplementary materials. Raw data is available upon request via Geert van den Bogaart (g.van.den.bogaart@rug.nl) and Sushil K. Mahata (smahata@health.ucsd.edu).

475 **Figure legends**

476

477 **Fig. 1. CgA is efficiently processed to CST in the colon and CST levels correlate**
478 **with Crohn's disease activity. (A)** TEM micrographs (n=3) showing enteroendocrine
479 cell DCV in colon of WT, CgA-KO and CST-KO mice, (**B**) fewer DCV in CgA-KO and CST-
480 KO mice (1-way ANOVA) but enlarged DCV in CST-KO mice and smaller DCV in CgA-
481 KO mice (>500 vesicles from 30 micrographs) (Kolmogorov-Smirnov test). DCV, dense
482 core vesicles; Nuc, nucleus. (**C**) CgA protein and CST peptide levels in colon of WT and
483 CST-KO mice. CgA levels are comparable between WT and CST-KO mice. CST level is
484 markedly higher in WT mice and is undetectable in CST-KO mice (n=6; Welch's *t* test).
485 (**D**) Expression of proteolytic genes (n=7). *Ctsl* and *Plg* are differentially expressed in
486 colon of CgA-KO and CST-KO mice (n=8; 1-way ANOVA). (**E**) CgA and CST levels in
487 EDTA-plasma of healthy donors (Control) and Crohn's disease patients (N=89) in
488 remission or flare-up (2-way ANOVA). Ns, not significant; **p<0.01; ***p<0.001.

489

490 **Fig. 2. Impaired epithelial barrier function in CST-KO mice.** (**A**) TEM micrographs
491 (n=3) showing tight junction (TJ), adherens junction (AJ), and desmosomes (Des). MV,
492 microvillus. (**B**) Morphometrical analyses (n=20-54) showing increased length and
493 diameter of TJ, AJ and Des in CST-KO mice (Welch's *t* test). (C) Differential expression
494 of genes in TJ (*Cldn2, Ocln, Marveld2, F11r*, and *Tjp1*), AJ (*Ctnna1*, *Ctnnb1*, and *Cdh1*)
495 and Des (*Dsg2*) in colon of CST-KO mice compared to WT mice (n=8; 2-way ANOVA or
496 Welch's *t* test). (D) Increased gut permeability as measured by FITC-dextran level in CST-
497 KO compared to WT mice (n=8; Welch's *t* test). *p<0.05; **p<0.01; ***p<0.001.

498

499 **Fig. 3. Increased gut inflammation in colon of CST-KO mice. (A)** TEM micrographs
500 (n=3) showing increased number of immune cells in colon of CST-KO mice. Arrows
501 indicate immune cells. Cap, capillary; Ec, enterocytes; Gc, goblet cells; LP, lamina
502 propria. (**B**) Flow cytometry study (n=5-10) shows increased number of macrophages
503 ($CD45^+CD11b^+Emr1^+$) and T cells ($CD45^+CD4^+$) in colon of CST-KO mice (n=5-10;
504 Welch's *t* test). (**C**) Increased expression of proinflammatory genes (*Tnfa, Ifng, Cxcl1,*
505 *Ccl2, Emr1, Itgam*, and *Itgax*), and (**D**) proinflammatory proteins (Tnfα, Ifnγ, Cxcl1, and

506 Ccl2) in colon of CST-KO mice (n=8; 2-way ANOVA). Decreased expression of (**E**) anti-
507 inflammatory genes (*Arg1, Il4, Tgfb1, Il10, Mrc1, Clec7a,* and *Clec10a*) (n=8; 2-way
508 ANOVA), and (**F**) anti-inflammatory protein (Il10) (n=8; Welch's *t* test) in colon of CST-
509 KO mice (n=8). (**G**) Increased expression of proinflammatory calprotectin gene and
510 protein in colon of CST-KO mice (n=5; Welch's *t* test). *p<0.05; **p<0.01; ***p<0.001.
511
512
513 **Fig. 4. Increased ratio of Firmicutes to Bacteriodetes in CST-KO mice. (A)** Principal
514 CoordiNATE Analysis (PCoA) of microbiome data using Bray-Curtis distance of species
515 composition and abundance in individual WT (blue) and CST-KO (red) mice. **(C-D)**
516 Microbiota composition of cecum of WT and CST-KO mice for main bacteria phyla **(B)**
517 and the geni within the *Bacteriodetes* **(C)** and *Firmicutes* **(D).**
518
519 **Fig. 5. Exogenous CST can rescue epithelial barrier function and inflammation in**
520 **CST-KO mice. (A)** Gut permeability as measured by FITC-Dextran plasma level in WT
521 and CST-KO mice treated with saline of CST (n=8; 2-way ANOVA). Relative mRNA
522 expression of genes involved in (**B**) tight junctions (*Cldn2*, *Ocln*, *Marveld2*, *F11r* and
523 *Tjp1*), (**C**) adherens junctions (*Ctnna1, Ctnnb1*, and *Cdh1*), and (**D**) desmosomes (*Dsg2*)
524 in colon of CST-KO mice treated with saline or CST (n=8; 2-way ANOVA or Welch's *t*
525 test). Decreased expression in colon of (**E**) proinflammatory genes (*Tnfa, Ifng, Cxcl1,*
526 *Ccl2, Emr1, Itgam*, and *Itgax*) and (**F**) proinflammatory proteins (Tnfα, Ifnγ, Cxcl1, and
527 Ccl2) after treatment of CST-KO mice with CST compared to treated with saline (n=8; 2-
528 way ANOVA). (**G**) Supplementation of CST-KO mice with CST increased colon
529 expression of (**G**) anti-inflammatory genes (*Arg1, Il4, Tgfb1, Il10, Mrc1, Clec7a,* and
530 *Clec10a*), and (**H**) anti-inflammatory protein (Il10) (n=8; 2-way ANOVA or Welch's *t* test).
531 Treatment of CST-KO mice with CST decreased colon expression of both (**I**) gene *s100a9*
532 coding for calprotectin subunit, and (**J**) calprotectin protein. *: P<0.05; **: P<0.01;
533 ***P<0.001.
534
535 **Fig. 6. Increased epithelial barrier function and lower inflammation in CgA-KO mice.**
536 **(A)** Electron microscopy micrographs of colon of WT and CgA-KO mice. TJ: tight junction.

537 AJ: adherens junction. Des: desmosomes. **(B)** Gut permeability as measured by FITC-
538 Dextran plasma level in WT and CgA-KO mice (n=7; Welch's *t* test). **(C)** Relative mRNA
539 expression of genes in tight junction (*Cldn2*, *Ocln*, *Marveld2*, *F11r,* and *Tjp1*) (n=8, 2-way
540 ANOVA), adherens junction (*Ctnna1, Ctnnb1*, and *Cdh1*) (n=8; 2-way ANOVA), and
541 desmosome (*Dsg2*) (n=8; Welch's *t* test) in colon of WT and CgA-KO mice. Comparable
542 expression of (**D**) proinflammatory genes (*Tnfa, Ifng, Cxcl1, Ccl2, Emr1, Itgam*, and *Itgax*),
543 and (**E**) proinflammatory proteins (Tnfα, Ifnγ, Cxcl1*,* and Ccl2) in colon of WT and CgA-
544 KO mice (n=8, 2-way ANOVA). Increased expression of **(F)** anti-inflammatory genes
545 (*Arg1, Tgfb1, Clec7a, and Clec10a*) and comparable expression of anti-inflammatory
546 genes (*Il4, Il10,* and *Mrc1*), and **(G)** anti-inflammatory protein (Il10) in colon of WT and
547 CgA-KO mice (n=8; 2-way ANOVA or Welch's *t* test). **(H)** Comparable expression of
548 *s100a9* gene and decreased expression of calprotectin protein in CgA-KO colon (n=5;
549 Welch's *t* test). **: P<0.01; ***P<0.001.
550
551 **Fig. 7. Altered microbiome composition in CgA-KO mice and CST and PST**
552 **oppositely regulate gut permeability. (A)** Microbiota composition of cecum of WT and
553 CgA-KO mice for main bacteria phyla and the geni within the Bacteriodetes and
554 Firmicutes. **(B)** Scheme of CgA indicating the positions of the peptide products vasostatin
555 1, PST, CST and serpinin. **(C)** Gut permeability as measured by FITC-Dextran plasma
556 levels in WT, CST-KO and CgA-KO mice treated with saline or CST (n=8; 2-way ANOVA)
557 and in CgA-KO mice treated with PST or a combination of PST and CST (n=8; 1-way
558 ANOVA). **(D)** Model of gut barrier regulation by CST and PST. ***P<0.001.
559
560
561

562 **References**

563

564 1. Sender R, Fuchs S, Milo R. Revised Estimates for the Number of Human and
565 Bacteria Cells in the Body. PLoS Biol 2016;14:e1002533.
566 2. Wassenaar TM, Zimmermann K. Lipopolysaccharides in Food, Food
567 Supplements, and Probiotics: Should We be Worried? Eur J Microbiol Immunol
568 (Bp) 2018;8:63-69.
569 3. Perez-Reytor D, Jana V, Pavez L, et al. Accessory Toxins of Vibrio Pathogens and
570 Their Role in Epithelial Disruption During Infection. Front Microbiol 2018;9:2248.
571 4. Sartor RB, Wu GD. Roles for Intestinal Bacteria, Viruses, and Fungi in
572 Pathogenesis of Inflammatory Bowel Diseases and Therapeutic Approaches.
573 Gastroenterology 2017;152:327-339 e4.
574 5. Meyer-Hoffert U, Hornef MW, Henriques-Normark B, et al. Secreted enteric
575 antimicrobial activity localises to the mucus surface layer. Gut 2008;57:764-71.
576 6. Chakaroun RM, Massier L, Kovacs P. Gut Microbiome, Intestinal Permeability, and
577 Tissue Bacteria in Metabolic Disease: Perpetrators or Bystanders? Nutrients
578 2020;12.
579 7. Buckley A, Turner JR. Cell Biology of Tight Junction Barrier Regulation and
580 Mucosal Disease. Cold Spring Harb Perspect Biol 2018;10.
581 8. Lutter L, Hoytema van Konijnenburg DP, Brand EC, Oldenburg B, van Wijk F. The
582 elusive case of human intraepithelial T cells in gut homeostasis and inflammation.
583 (2018) Nat. Rev. Gastroenterol. Hepatol. 15:637-49.
584 9. Weber CR, Raleigh DR, Su L, et al. Epithelial myosin light chain kinase activation
585 induces mucosal interleukin-13 expression to alter tight junction ion selectivity. J
586 Biol Chem 2010;285:12037-46.
587 10. Marchiando AM, Shen L, Graham WV, et al. Caveolin-1-dependent occludin
588 endocytosis is required for TNF-induced tight junction regulation in vivo. J Cell Biol
589 2010;189:111-26.
590 11. Scharl M, Paul G, Barrett KE, et al. AMP-activated protein kinase mediates the
591 interferon-gamma-induced decrease in intestinal epithelial barrier function. J Biol
592 Chem 2009;284:27952-63.
593 12. Ye D, Ma I, Ma TY. Molecular mechanism of tumor necrosis factor-alpha
594 modulation of intestinal epithelial tight junction barrier. Am J Physiol Gastrointest
595 Liver Physiol 2006;290:G496-504.
596 13. Winkler H, Fischer-Colbrie R. The chromogranins A and B: the first 25 years and
597 future perspectives. Neuroscience 1992;49:497-528.
598 14. Bartolomucci A, Possenti R, Mahata SK, et al. The extended granin family:
599 structure, function, and biomedical implications. Endocr Rev 2011;32:755-97.
600 15. Mahata SK, Corti A. Chromogranin A and its fragments in cardiovascular,
601 immunometabolic, and cancer regulation. Ann N Y Acad Sci 2019;1455:34-58.
602 16. Zhang X, Zhang H, Shen B, et al. Chromogranin-A Expression as a Novel
603 Biomarker for Early Diagnosis of Colon Cancer Patients. Int J Mol Sci 2019;20.
604 17. El-Salhy M, Patcharatrakul T, Hatlebakk JG, et al. Chromogranin A cell density in
605 the large intestine of Asian and European patients with irritable bowel syndrome.
606 Scand J Gastroenterol 2017;52:691-697.

607 18. Mahata SK, O'Connor DT, Mahata M, et al. Novel autocrine feedback control of
608 catecholamine release. A discrete chromogranin A fragment is a noncompetitive
609 nicotinic cholinergic antagonist. J Clin Invest 1997;100:1623-33.
610 19. Tatemoto K, Efendic S, Mutt V, et al. Pancreastatin, a novel pancreatic peptide
611 that inhibits insulin secretion. Nature 1986;324:476-8.
612 20. Curry WJ, Shaw C, Johnston CF, et al. Isolation and primary structure of a novel
613 chromogranin A-derived peptide, WE-14, from a human midgut carcinoid tumour.
614 FEBS Lett 1992;301:319-21.
615 21. Aardal S, Helle KB, Elsayed S, et al. Vasostatins, comprising the N-terminal
616 domain of chromogranin A, suppress tension in isolated human blood vessel
617 segments. J Neuroendocrinol 1993;5:405-12.
618 22. Koshimizu H, Cawley NX, Kim T, et al. Serpinin: a novel chromogranin A-derived,
619 secreted peptide up-regulates protease nexin-1 expression and granule
620 biogenesis in endocrine cells. Mol Endocrinol 2011;25:732-44.
621 23. Bandyopadhyay GK, Lu M, Avolio E, et al. Pancreastatin-dependent inflammatory
622 signaling mediates obesity-induced insulin resistance. Diabetes 2015;64:104-16.
623 24. Bandyopadhyay GK, Vu CU, Gentile S, et al. Catestatin (chromogranin A(352-
624 372)) and novel effects on mobilization of fat from adipose tissue through
625 regulation of adrenergic and leptin signaling. J Biol Chem 2012;287:23141-51.
626 25. Bandyopadhyay GK, Mahata SK. Chromogranin A Regulation of Obesity and
627 Peripheral Insulin Sensitivity. Front Endocrinol (Lausanne) 2017;8:20.
628 26. Ying W, Mahata S, Bandyopadhyay GK, et al. Catestatin Inhibits Obesity-Induced
629 Macrophage Infiltration and Inflammation in the Liver and Suppresses Hepatic
630 Glucose Production, Leading to Improved Insulin Sensitivity. Diabetes
631 2018;67:841-848.
632 27. Kojima M, Ozawa N, Mori Y, et al. Catestatin Prevents Macrophage-Driven
633 Atherosclerosis but Not Arterial Injury-Induced Neointimal Hyperplasia. Thromb
634 Haemost 2018;118:182-194.
635 28. Gupta, J & Nebreda, A. Analysis of Intestinal Permeability in Mice. (2014) BIO-
636 PROTOCOL 4.
637 29. Pasqua T, Mahata S, Bandyopadhyay GK, et al. Impact of Chromogranin A
638 deficiency on catecholamine storage, catecholamine granule morphology and
639 chromaffin cell energy metabolism in vivo. Cell Tissue Res 2016;363:693-712.
640 30. Sahu BS, Mahata S, Bandyopadhyay K, et al. Catestatin regulates vesicular
641 quanta through modulation of cholinergic and peptidergic (PACAPergic)
642 stimulation in PC12 cells. Cell Tissue Res 2019;376:51-70.
643 31. Hasan, et al. Microbial Community Profiling of Human Saliva Using Shotgun
644 Metagenomic Sequencing. (2014) PLoS One 9:e97699
645 32. Lax, et al. Longitudinal analysis of microbial interaction between humans and the
646 indoor environment. (2014) Science 345:1048-52
647 33. Ponnusamy, et al. Cross-talk among flesh-eating Aeromonas hydrophila strains in
648 mixed infection leading to necrotizing fasciitis. Proc. Natl. Acad. Sci. U. S. A. (2016)
649 113:722–7
650 34. Mahapatra NR, O'Connor DT, Vaingankar SM, et al. Hypertension from targeted
651 ablation of chromogranin A can be rescued by the human ortholog. J Clin Invest
652 2005;115:1942-52.

653 35. Ying W, Tang K, Avolio E, et al. Catestatin (CST) is a key mediator of the
654 immunoendocrine regulation of cardiovascular function. BioRxiv 2020;2020.
655 36. Parmer RJ, Mahata M, Gong Y, et al. Processing of chromogranin A by plasmin
656 provides a novel mechanism for regulating catecholamine secretion. J Clin Invest
657 2000;106:907-915.
658 37. Jiang Q, Taupenot L, Mahata SK, et al. Proteolytic cleavage of chromogranin A
659 (CgA) by plasmin: selective liberation of a specific bioactive CgA fragment that
660 regulates catecholamine release. J Biol Chem 2001;276:25022-25029.
661 38. Biswas N, Vaingankar SM, Mahata M, et al. Proteolytic cleavage of human
662 chromogranin a containing naturally occurring catestatin variants: differential
663 processing at catestatin region by plasmin. Endocrinology 2008;149:749-57.
664 39. Biswas N, Rodriguez-Flores JL, Courel M, et al. Cathepsin L Co-Localizes with
665 Chromogranin a in Chromaffin Vesicles to Generate Active Peptides.
666 Endocrinology 2009;150:3547-57.
667 40. O'Connor DT, Kailasam MT, Kennedy BP, et al. Early decline in the catecholamine
668 release-inhibitory peptide catestatin in humans at genetic risk of hypertension. J
669 Hypertens 2002;20:1335-45.
670 41. O'Connor DT, Zhu G, Rao F, et al. Heritability and genome-wide linkage in US and
671 australian twins identify novel genomic regions controlling chromogranin a:
672 implications for secretion and blood pressure. Circulation 2008;118:247-57.
673 42. Chen Y, Wang X, Yang C, et al. Decreased circulating catestatin levels are
674 associated with coronary artery disease: The emerging anti-inflammatory role.
675 Atherosclerosis 2019;281:78-88.
676 43. Durakoglugil ME, Ayaz T, Kocaman SA, et al. The relationship of plasma catestatin
677 concentrations with metabolic and vascular parameters in untreated hypertensive
678 patients: Influence on high-density lipoprotein cholesterol. Anatol J Cardiol
679 2015;15:577-85.
680 44. Ottesen AH, Carlson CR, Louch WE, et al. Glycosylated Chromogranin A in Heart
681 Failure: Implications for Processing and Cardiomyocyte Calcium Homeostasis.
682 Circ Heart Fail 2017;10.
683 45. Zissimopoulos A, Vradelis S, Konialis M, et al. Chromogranin A as a biomarker of
684 disease activity and biologic therapy in inflammatory bowel disease: a prospective
685 observational study. Scand J Gastroenterol 2014;49:942-9.
686 46. Sidhu, et al. Elevated Serum Chromogranin A in Irritable Bowel Syndrome (IBS)
687 and Inflammatory Bowel Disease (IBD): A Shared Model for Pathogenesis?
688 Inflamm. Bowel Dis. 2010;16:361–540.
689 47. Sciola, et al. Plasma Chromogranin A in patients with inflammatory bowel disease.
690 Inflamm. Bowel Dis. 2009;15:867.
691 48. Wagner, et al. Increased Fecal Levels of Chromogranin A, Chromogranin B, and
692 Secretoneurin in Collagenous Colitis. Inflammation 2013;36:855.
693 49. Strid, et al. Fecal chromogranins and secretogranins are increased in patients with
694 ulcerative colitis but are not associated with disease activity. J. Crohn's Colitis
695 2013;7:e615.
696 50. Zivkovic, et al. Serum Catestatin Levels and Arterial Stiffness Parameters Are
697 Increased in Patients with Inflammatory Bowel Disease. J. Clin. Med. 2020;9:628.

51. Amasheh S, Meiri N, Gitter AH, et al. Claudin-2 expression induces cation-selective channels in tight junctions of epithelial cells. J Cell Sci 2002;115:4969-76.
52. Adams RB, Planchon SM, Roche JK. IFN-gamma modulation of epithelial barrier function. Time course, reversibility, and site of cytokine binding. J Immunol 1993;150:2356-63.
53. Ma TY, Iwamoto GK, Hoa NT, et al. TNF-alpha-induced increase in intestinal epithelial tight junction permeability requires NF-kappa B activation. Am J Physiol Gastrointest Liver Physiol 2004;286:G367-76.
54. Howe KL, Reardon C, Wang A, et al. Transforming growth factor-beta regulation of epithelial tight junction proteins enhances barrier function and blocks enterohemorrhagic Escherichia coli O157:H7-induced increased permeability. Am J Pathol 2005;167:1587-97.
55. Costa F, Mumolo MG, Bellini M, et al. Role of faecal calprotectin as non-invasive marker of intestinal inflammation. Dig Liver Dis 2003;35:642-7.
56. Zhernakova A, Kurilshikov A, Bonder MJ, et al. Population-based metagenomics analysis reveals markers for gut microbiome composition and diversity. Science 2016;352:565-9.
57. Costa F, Mumolo MG, Ceccarelli L, et al. Calprotectin is a stronger predictive marker of relapse in ulcerative colitis than in Crohn's disease. Gut 2005;54:364-8.
58. Bonfrate L, Tack J, Grattagliano I, et al. Microbiota in health and irritable bowel syndrome: current knowledge, perspectives and therapeutic options. Scand J Gastroenterol 2013;48:995-1009.
59. Scaldaferri F, Gerardi V, Lopetuso LR, et al. Gut microbial flora, prebiotics, and probiotics in IBD: their current usage and utility. Biomed Res Int 2013;2013:435268.
60. Rabbi, et al. Human Catestatin Alters Gut Microbiota Composition in Mice. (2016) Front. Microbiol. 7:2151.
61. Cani PD, Osto M, Geurts L, et al. Involvement of gut microbiota in the development of low-grade inflammation and type 2 diabetes associated with obesity. Gut Microbes 2012;3:279-88.
62. Michielan A, D'Inca R. Host-microbiome interaction in Crohn's disease: A familiar or familial issue? World J Gastrointest Pathophysiol 2015;6:159-68.
63. Packey CD, Sartor RB. Commensal bacteria, traditional and opportunistic pathogens, dysbiosis and bacterial killing in inflammatory bowel diseases. Curr Opin Infect Dis 2009;22:292-301.
64. Maloy KJ, Powrie F. Intestinal homeostasis and its breakdown in inflammatory bowel disease. Nature 2011;474:298-306.
65. Rabbi MF, Eissa N, Munyaka PM, et al. Reactivation of Intestinal Inflammation Is Suppressed by Catestatin in a Murine Model of Colitis via M1 Macrophages and Not the Gut Microbiota. Front Immunol 2017;8:985.
66. Rabbi MF, Labis B, Metz-Boutigue MH, et al. Catestatin decreases macrophage function in two mouse models of experimental colitis. Biochem Pharmacol 2014;89:386-98.

742 67. Eissa N, Kermarrec L, Hendy GN, et al. Pancreastatin worsens intestinal
743 inflammation by inducing classically activated macrophages (M1) through
744 suppression of STAT3. J Can Assoc Gastroenterol 2018;1 149-150.
745 68. Lee JC, Taylor CV, Gaucher SP, et al. Primary sequence characterization of
746 catestatin intermediates and peptides defines proteolytic cleavage sites utilized for
747 converting chromogranin a into active catestatin secreted from neuroendocrine
748 chromaffin cells. Biochemistry 2003;42:6938-46.
749 69. Benyamin B, Maihofer AX, Schork AJ, et al. Identification of novel loci affecting
750 circulating chromogranins and related peptides. Hum Mol Genet 2016.
751 70. Gayen JR, Saberi M, Schenk S, et al. A novel pathway of insulin sensitivity in
752 chromogranin a null mice: A crucial role for pancreastatin in glucose homeostasis.
753 J Biol Chem 2009;284:28498-28509.
754 71. Dasgupta A, Bandyopadhyay GK, Ray I, et al. Catestatin improves insulin
755 sensitivity by attenuating endoplasmic reticulum stress: In vivo and in silico
756 validation. Comput Struct Biotechnol J 2020;18:464-481.
757 72. Al-Sadi R, Ye D, Dokladny K, et al. Mechanism of IL-1beta-induced increase in
758 intestinal epithelial tight junction permeability. J Immunol 2008;180:5653-61.
759 73. Capaldo CT, Nusrat A. Cytokine regulation of tight junctions. Biochim Biophys Acta
760 2009;1788:864-71.
761 74. Su L, Nalle SC, Shen L, et al. TNFR2 activates MLCK-dependent tight junction
762 dysregulation to cause apoptosis-mediated barrier loss and experimental colitis.
763 Gastroenterology 2013;145:407-15.
764 75. Mankertz J, Amasheh M, Krug SM, et al. TNFalpha up-regulates claudin-2
765 expression in epithelial HT-29/B6 cells via phosphatidylinositol-3-kinase signaling.
766 Cell Tissue Res 2009;336:67-77.
767 76. Suzuki T, Yoshinaga N, Tanabe S. Interleukin-6 (IL-6) regulates claudin-2
768 expression and tight junction permeability in intestinal epithelium. J Biol Chem
769 2011;286:31263-71.
770 77. Saia RS, Ribeiro AB, Giusti H. Cholecystokinin Modulates the Mucosal
771 Inflammatory Response and Prevents the Lipopolysaccharide-Induced Intestinal
772 Epithelial Barrier Dysfunction. Shock 2020;53:242-251.
773 78. Wu R, Dong W, Qiang X, et al. Orexigenic hormone ghrelin ameliorates gut barrier
774 dysfunction in sepsis in rats. Crit Care Med 2009;37:2421-6.
775 79. Wu R, Dong W, Cui X, et al. Ghrelin down-regulates proinflammatory cytokines in
776 sepsis through activation of the vagus nerve. Ann Surg 2007;245:480-6.
777 80. Drucker DJ, Habener JF, Holst JJ. Discovery, characterization, and clinical
778 development of the glucagon-like peptides. J Clin Invest 2017;127:4217-4227.
779 81. Ottaway CA, Lewis DL, Asa SL. Vasoactive intestinal peptide-containing nerves in
780 Peyer's patches. Brain Behav Immun 1987;1:148-58.
781 82. Keita AV, Carlsson AH, Cigehn M, et al. Vasoactive intestinal polypeptide
782 regulates barrier function via mast cells in human intestinal follicle-associated
783 epithelium and during stress in rats. Neurogastroenterol Motil 2013;25:e406-17.
784 83. Izu LT, McCulle SL, Ferreri-Jacobia MT, et al. Vasoactive intestinal peptide-
785 stimulated Cl- secretion: activation of cAMP-dependent K+ channels. J Membr Biol
786 2002;186:145-57.

84. Conlin VS, Wu X, Nguyen C, et al. Vasoactive intestinal peptide ameliorates intestinal barrier disruption associated with Citrobacter rodentium-induced colitis. Am J Physiol Gastrointest Liver Physiol 2009;297:G735-50.
85. Dethlefsen L, McFall-Ngai M, Relman DA. An ecological and evolutionary perspective on human-microbe mutualism and disease. Nature 2007;449:811-8.
86. Lemichez E, Lecuit M, Nassif X, et al. Breaking the wall: targeting of the endothelium by pathogenic bacteria. Nat Rev Microbiol 2010;8:93-104.
87. Chin AC, Flynn AN, Fedwick JP, et al. The role of caspase-3 in lipopolysaccharide-mediated disruption of intestinal epithelial tight junctions. Can J Physiol Pharmacol 2006;84:1043-50.
88. Dao MC, Everard A, Aron-Wisnewsky J, et al. Akkermansia muciniphila and improved metabolic health during a dietary intervention in obesity: relationship with gut microbiome richness and ecology. Gut 2016;65:426-36.
89. Everard A, Belzer C, Geurts L, et al. Cross-talk between Akkermansia muciniphila and intestinal epithelium controls diet-induced obesity. Proc Natl Acad Sci U S A 2013;110:9066-71.
90. Cani PD, Amar J, Iglesias MA, et al. Metabolic endotoxemia initiates obesity and insulin resistance. Diabetes 2007;56:1761-72.
91. Moreira AP, Texeira TF, Ferreira AB, et al. Influence of a high-fat diet on gut microbiota, intestinal permeability and metabolic endotoxaemia. Br J Nutr 2012;108:801-9.
92. Johne B, Fagerhol MK, Lyberg T, et al. Functional and clinical aspects of the myelomonocyte protein calprotectin. Mol Pathol 1997;50:113-23.
93. von Martels JZH, Bourgonje AR, Harmsen HJM, et al. Assessing intestinal permeability in Crohn's disease patients using orally administered 52Cr-EDTA. PLoS One 2019;14:e0211973.
94. Mulak A, Koszewicz M, Panek-Jeziorna M, et al. Fecal Calprotectin as a Marker of the Gut Immune System Activation Is Elevated in Parkinson's Disease. Front Neurosci 2019;13:992.
95. Berstad A, Arslan G, Folvik G. Relationship between intestinal permeability and calprotectin concentration in gut lavage fluid. Scand J Gastroenterol 2000;35:64-9.
96. Turpin W, Lee SH, Raygoza Garay JA, et al. Increased Intestinal Permeability is Associated with Later Development of Crohn's Disease. Gastroenterology 2020.

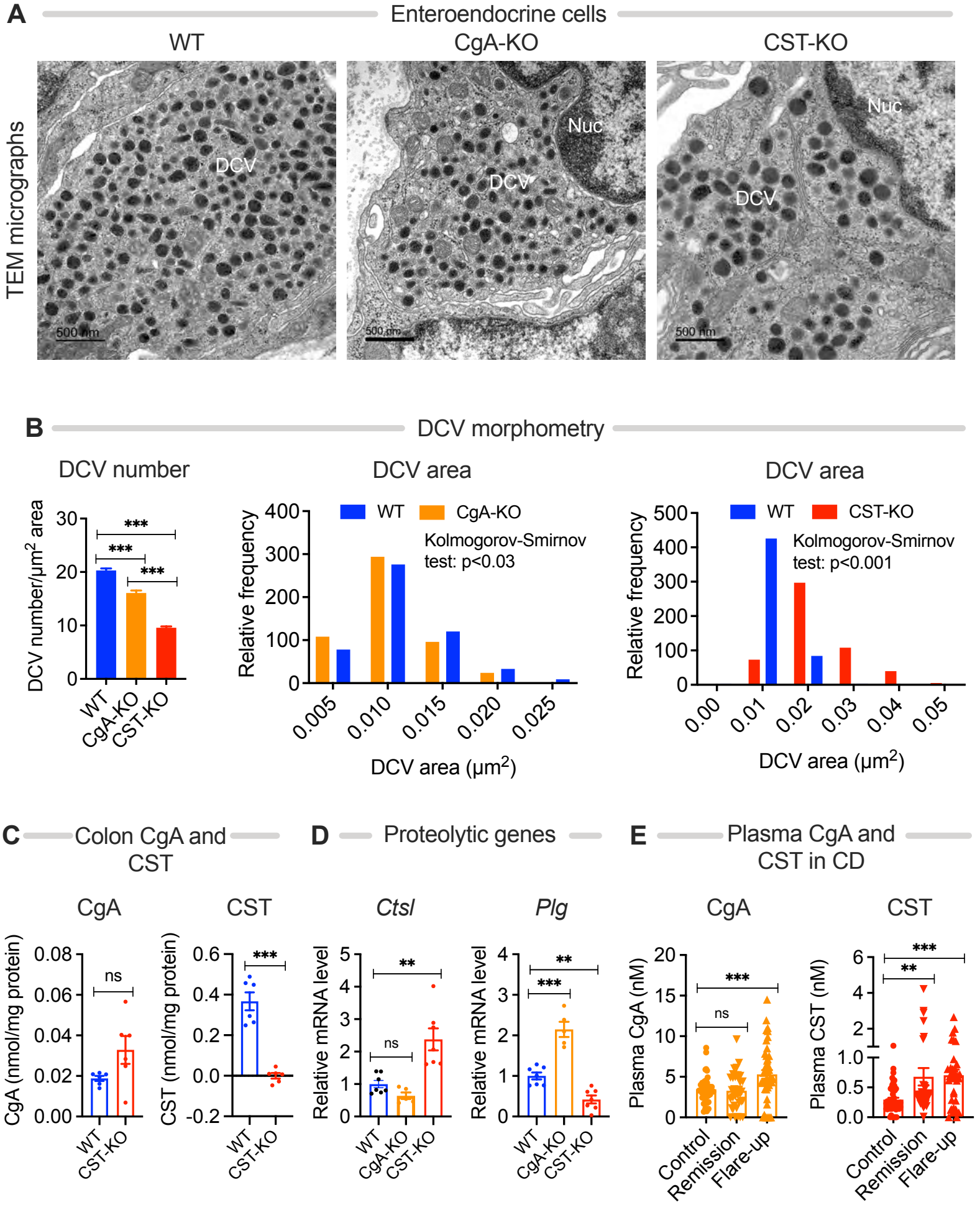
A
Enteroendocrine cells
WT
CgA-KO
CST-KO
TEM micrographs
DCV
Nuc
500 nm
B
DCV morphometry
DCV number
DCV number/μm² area
***
WT
CgA-KO
CST-KO
DCV area
Relative frequency
Kolmogorov-Smirnov test: p<0.03
DCV area (μm²)
Kolmogorov-Smirnov test: p<0.001
C
Colon CgA and CST
CgA
CST
CgA (nmol/mg protein)
CST (nmol/mg protein)
ns
D
Proteolytic genes
Ctsl
Plg
Relative mRNA level
**
E
Plasma CgA and CST in CD
Plasma CgA (nM)
Plasma CST (nM)
Control
Remission
Flare-up

Fig. 1

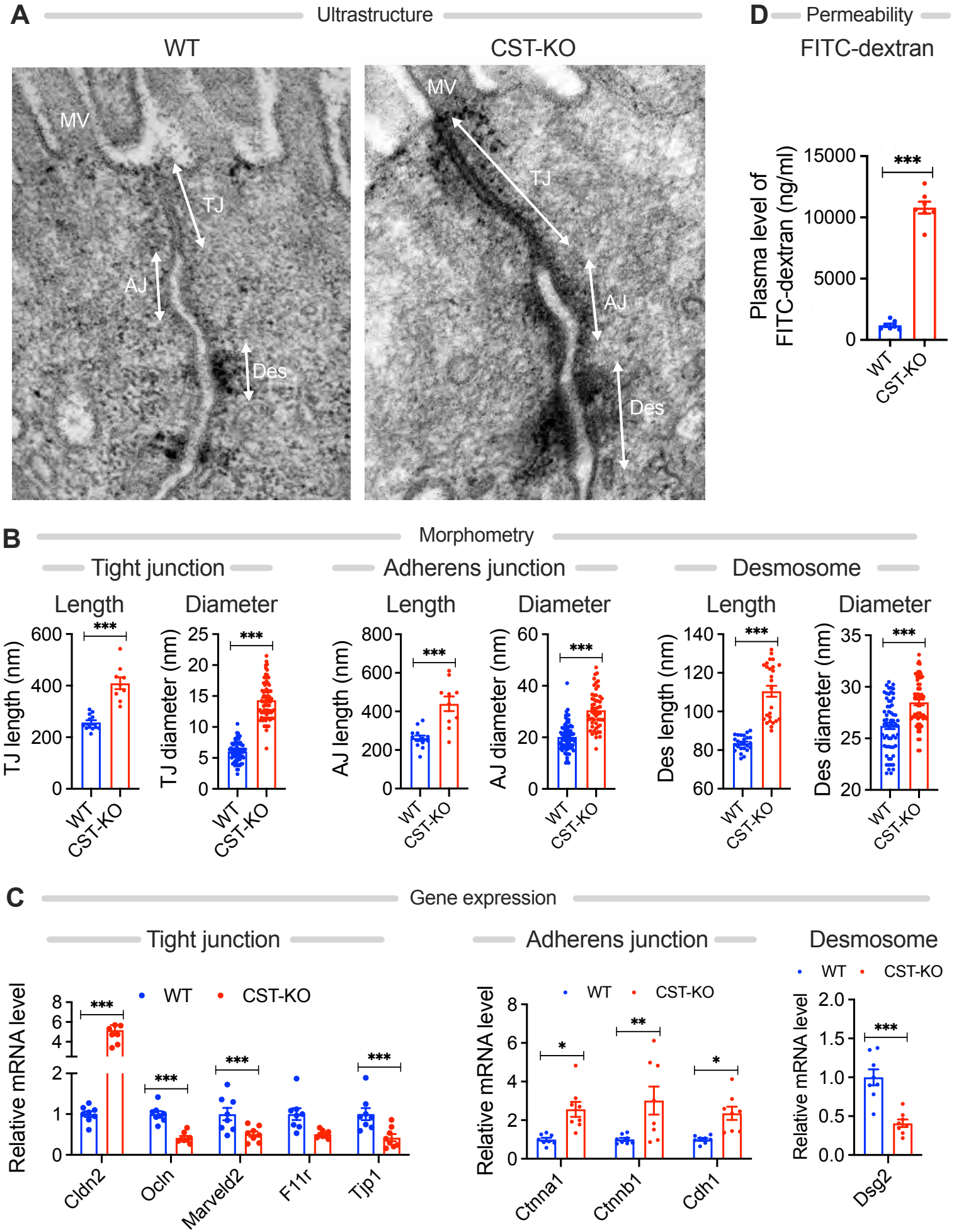
A
Ultrastructure
WT
CST-KO
MV
TJ
AJ
Des
D
Permeability
FITC-dextran
Plasma level of FITC-dextran (ng/ml)
15000
10000
5000
0
***
WT
CST-KO
B
Morphometry
Tight junction
Adherens junction
Desmosome
Length
Diameter
TJ length (nm)
TJ diameter (nm)
AJ length (nm)
AJ diameter (nm)
Des length (nm)
Des diameter (nm)
C
Gene expression
Relative mRNA level
Cldn2
Ocln
Marveld2
F11r
Tjp1
Ctnna1
Ctnnb1
Cdh1
Dsg2
*
**

Fig. 2

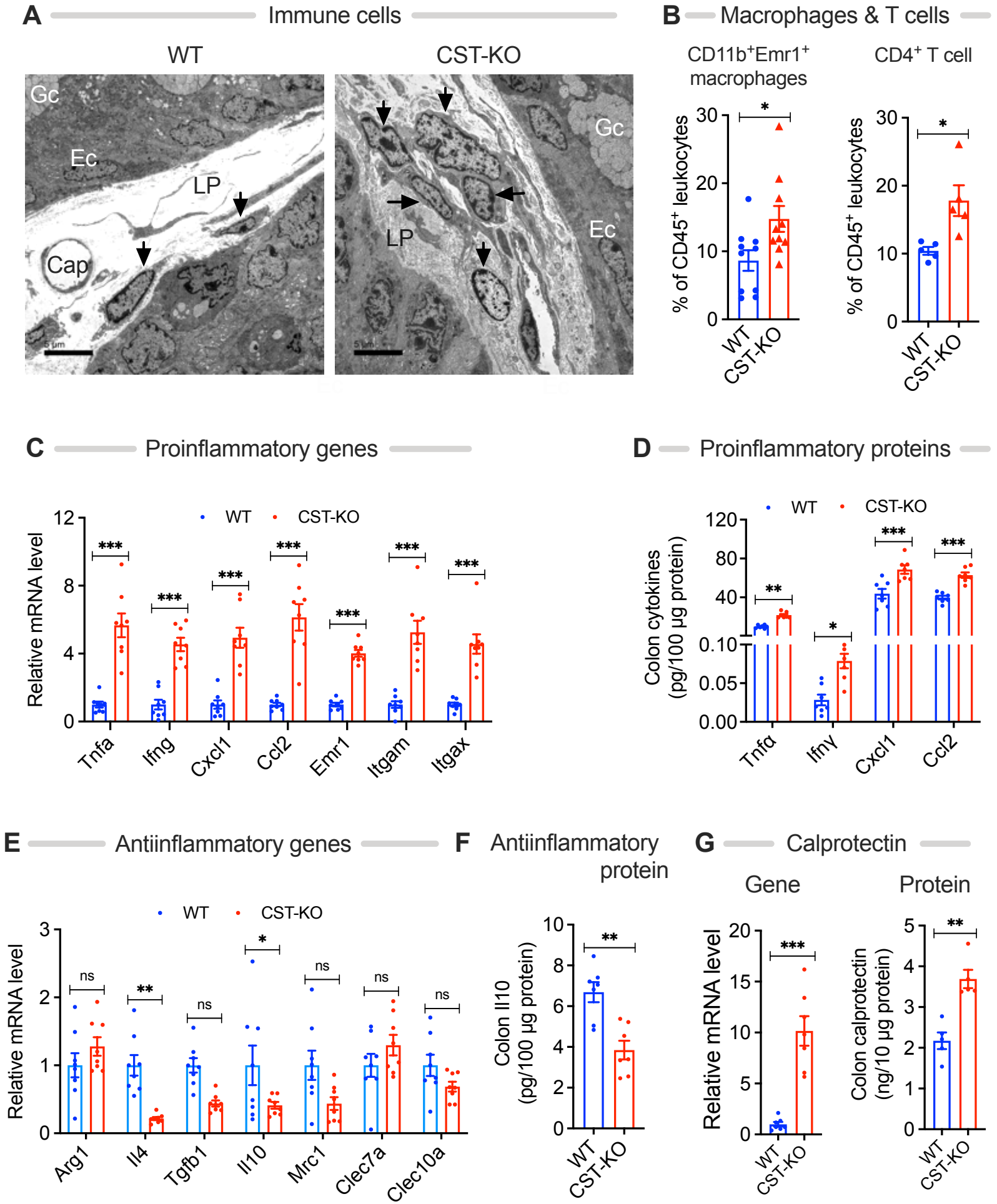
A
Immune cells
WT
CST-KO
Gc
Ec
LP
Cap
B
Macrophages & T cells
CD11b+Emr1+ macrophages
CD4+ T cell
% of CD45+ leukocytes
WT
CST-KO
C
Proinflammatory genes
Relative mRNA level
Tnfa
Ifng
Cxcl1
Ccl2
Emr1
Itgam
Itgax
D
Proinflammatory proteins
Colon cytokines (pg/100 µg protein)
Tnfα
Ifnγ
E
Antiinflammatory genes
Arg1
Il4
Tgfb1
Il10
Mrc1
Clec7a
Clec10a
ns
F
Antiinflammatory protein
Colon Il10 (pg/100 µg protein)
G
Calprotectin
Gene
Protein
Colon calprotectin (ng/10 µg protein)

Fig. 3

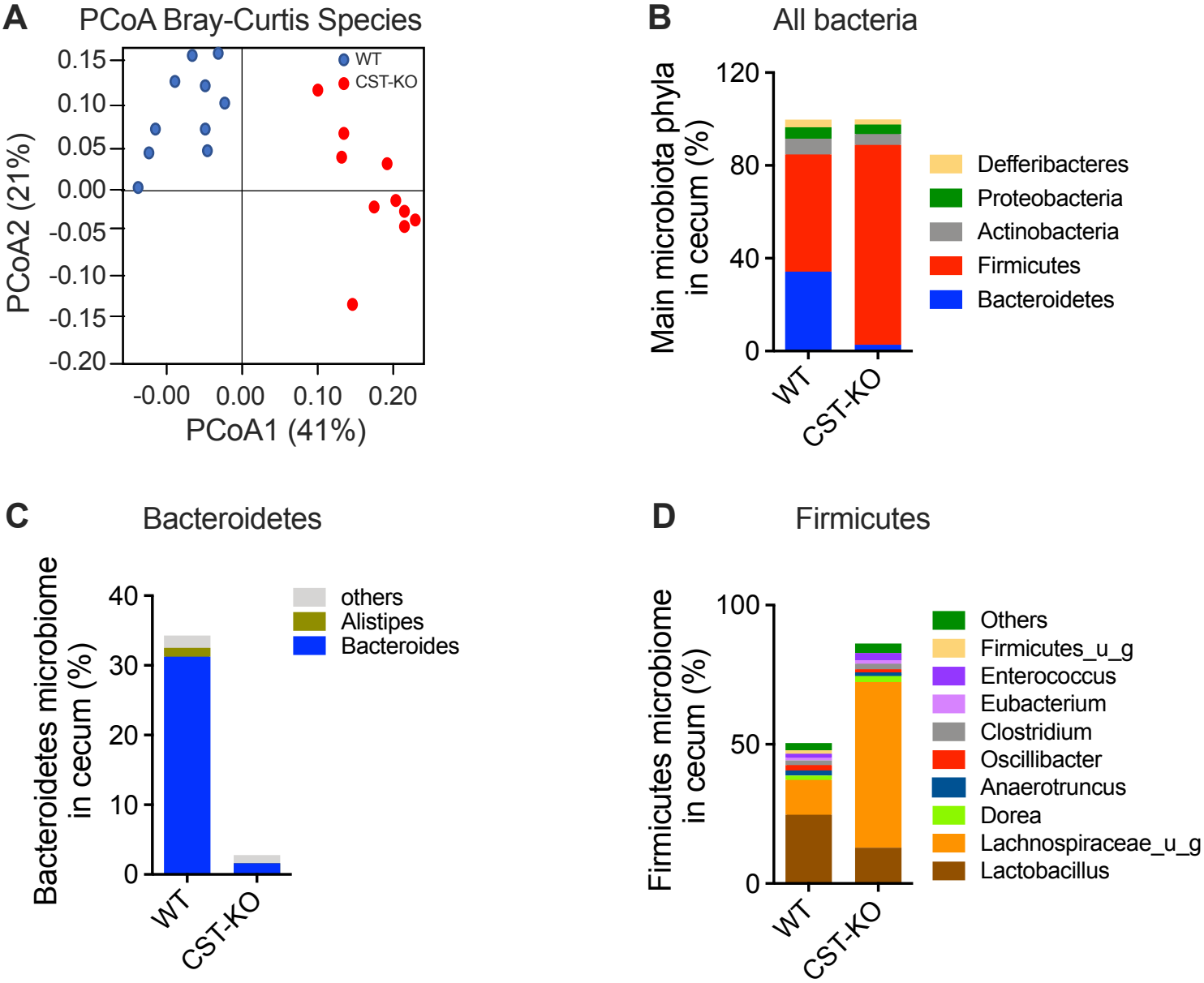
A
PCoA Bray-Curtis Species
WT
CST-KO
PCoA2 (21%)
PCoA1 (41%)
0.15
0.10
0.05
0.00
-0.05
-0.10
-0.15
-0.20
-0.00
0.00
0.10
0.20
B
All bacteria
Main microbiota phyla in cecum (%)
120
80
40
0
WT
CST-KO
Defferibacteres
Proteobacteria
Actinobacteria
Firmicutes
Bacteroidetes
C
Bacteroidetes
Bacteroidetes microbiome in cecum (%)
40
30
20
10
0
WT
CST-KO
others
Alistipes
Bacteroides
D
Firmicutes
Firmicutes microbiome in cecum (%)
100
50
0
WT
CST-KO
Others
Firmicutes_u_g
Enterococcus
Eubacterium
Clostridium
Oscillibacter
Anaerotruncus
Dorea
Lachnospiraceae_u_g
Lactobacillus

Fig. 4

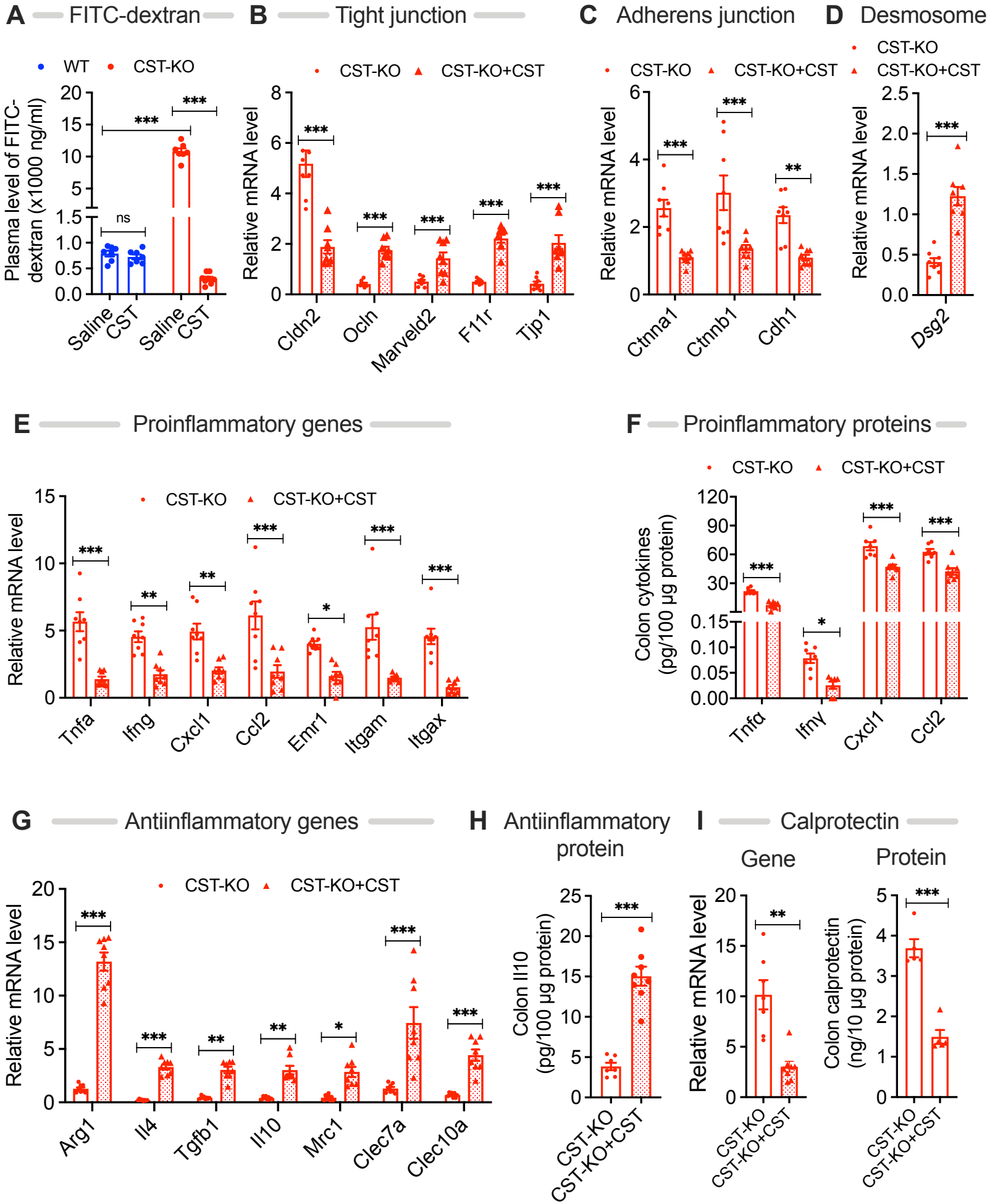
A
FITC-dextran
WT
CST-KO
Plasma level of FITC-dextran (x1000 ng/ml)
Saline
CST
Saline
CST
B
Tight junction
CST-KO
CST-KO+CST
Relative mRNA level
Cldn2
Ocln
Marveld2
F11r
Tjp1
C
Adherens junction
Ctnna1
Ctnnb1
Cdh1
D
Desmosome
Dsg2
E
Proinflammatory genes
Tnfa
Ifng
Cxcl1
Ccl2
Emr1
Itgam
Itgax
F
Proinflammatory proteins
Colon cytokines (pg/100 μg protein)
Tnfα
Ifnγ
Cxcl1
Ccl2
G
Antiinflammatory genes
Arg1
Il4
Tgfb1
Il10
Mrc1
Clec7a
Clec10a
H
Antiinflammatory protein
Colon Il10 (pg/100 μg protein)
I
Calprotectin
Gene
Protein
Colon calprotectin (ng/10 μg protein)

Fig. 5

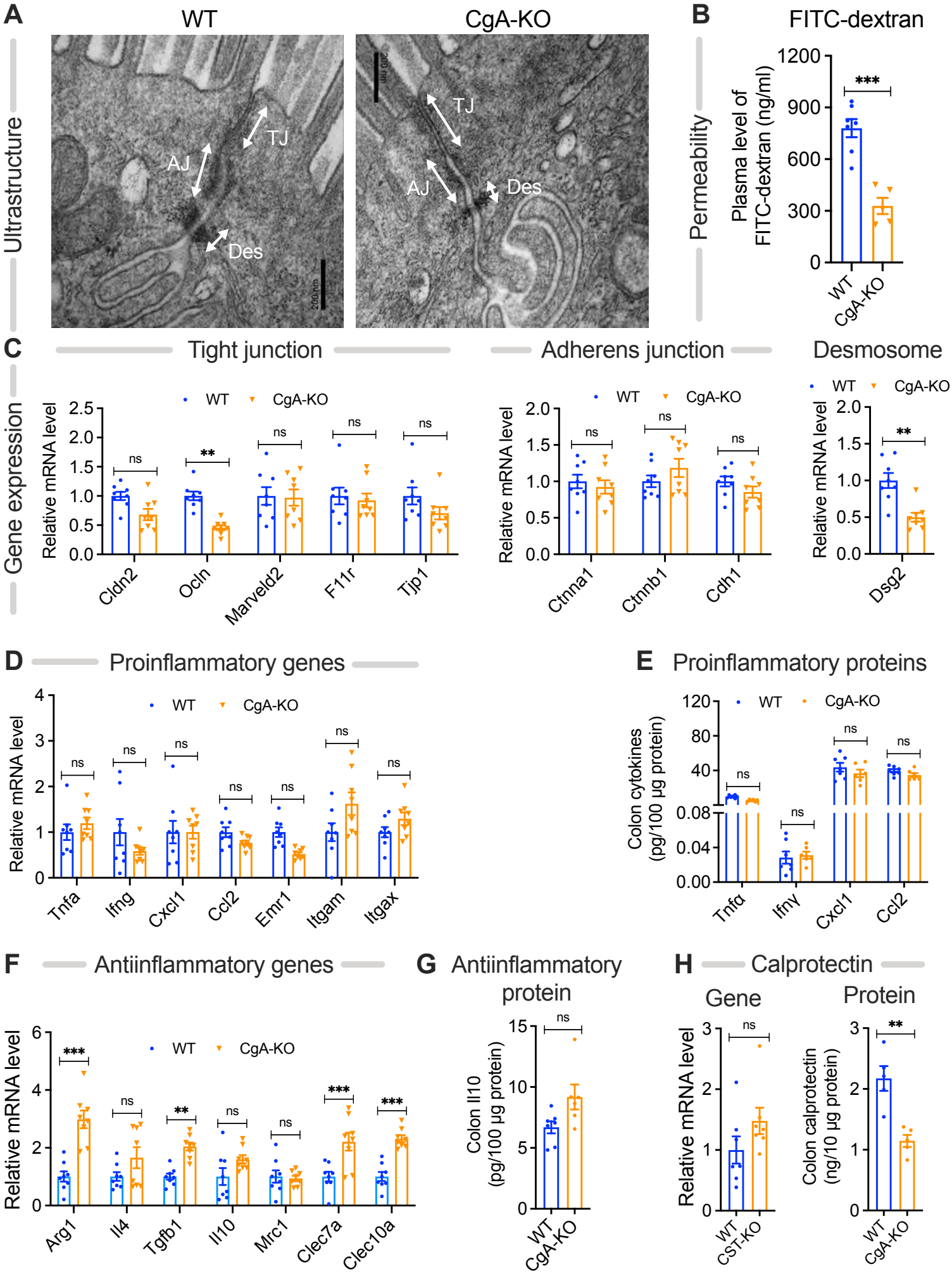
A
WT
CgA-KO
Ultrastructure
TJ
AJ
Des
200 nm
B
FITC-dextran
Permeability
Plasma level of FITC-dextran (ng/ml)
1200
900
600
300
0
***
WT
CgA-KO
C
Gene expression
Tight junction
Adherens junction
Desmosome
Relative mRNA level
Cldn2
Ocln
Marveld2
F11r
Tjp1
Ctnna1
Ctnnb1
Cdh1
Dsg2
ns
**
D
Proinflammatory genes
Tnfa
Ifng
Cxcl1
Ccl2
Emr1
Itgam
Itgax
E
Proinflammatory proteins
Colon cytokines (pg/100 µg protein)
Tnfα
Ifnγ
F
Antiinflammatory genes
Arg1
Il4
Tgfb1
Il10
Mrc1
Clec7a
Clec10a
***
G
Antiinflammatory protein
Colon Il10 (pg/100 µg protein)
H
Calprotectin
Gene
Protein
Colon calprotectin (ng/10 µg protein)
CST-KO

Fig. 6

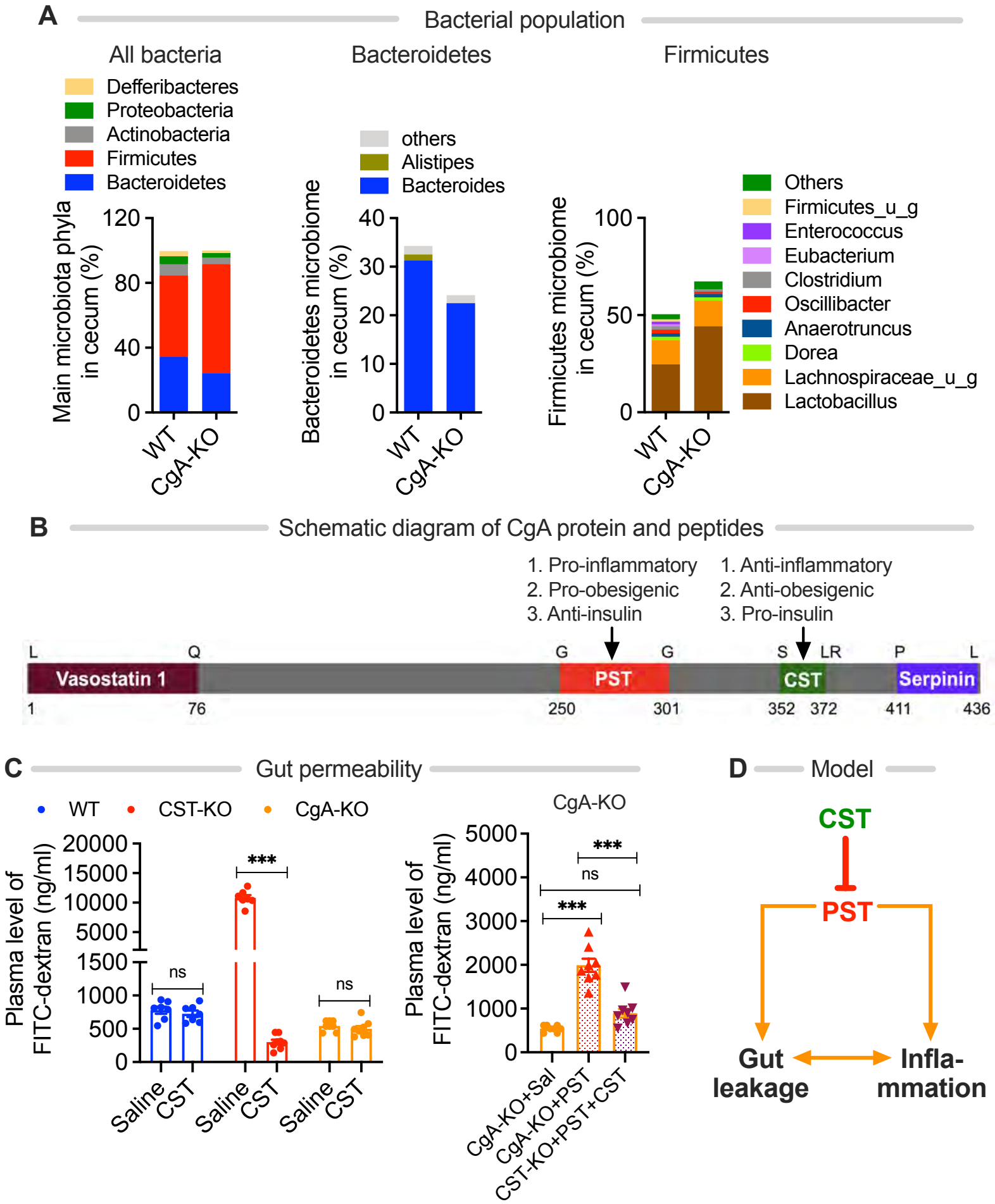
A
Bacterial population
All bacteria
Bacteroidetes
Firmicutes
Defferibacteres
Proteobacteria
Actinobacteria
Firmicutes
Bacteroidetes
Main microbiota phyla in cecum (%)
120
80
40
0
WT
CgA-KO
others
Alistipes
Bacteroides
Bacteroidetes microbiome in cecum (%)
40
30
20
10
0
WT
CgA-KO
Firmicutes microbiome in cecum (%)
100
50
0
WT
CgA-KO
Others
Firmicutes_u_g
Enterococcus
Eubacterium
Clostridium
Oscillibacter
Anaerotruncus
Dorea
Lachnospiraceae_u_g
Lactobacillus
B
Schematic diagram of CgA protein and peptides
1. Pro-inflammatory
2. Pro-obesigenic
3. Anti-insulin
1. Anti-inflammatory
2. Anti-obesigenic
3. Pro-insulin
L
Q
G
G
S
LR
P
L
Vasostatin 1
PST
CST
Serpinin
1
76
250
301
352
372
411
436
C
Gut permeability
WT
CST-KO
CgA-KO
Plasma level of FITC-dextran (ng/ml)
20000
15000
10000
5000
1500
1000
500
0
ns
***
ns
Saline
CST
Saline
CST
Saline
CST
CgA-KO
Plasma level of FITC-dextran (ng/ml)
5000
4000
3000
2000
1000
0
***
ns
***
CgA-KO+Sal
CgA-KO+PST
CST-KO+PST+CST
D
Model
CST
PST
Gut leakage
Infla-mmation

Fig. 7